Connection coefficients for cold plasma wave propagation near metallic surfaces

2013 Plasma Phys. Control. Fusion 55 055001

(http://iopscience.iop.org/0741-3335/55/5/055001)

Plasma Phys. Control. Fusion **55** (2013) 055001 (17pp) doi:10.1088/0741-3335/55/5/055001

Connection coefficients for cold plasma wave propagation near metallic surfaces

Dirk Van Eester[1], **Kristel Crombé**[1,2] **and Volodymyr Kyrytsya**[1]

[1] Laboratorium voor Plasmafysica-Laboratoire de Physique des Plasmas, Association 'EURATOM-Belgian State', Trilateral Euregio Cluster, Renaissancelaan 30 Avenue de la Renaissance, B-1000, Brussels, Belgium
[2] Department of Applied Physics, Ghent University, Sint-Pietersnienwstraat 41 B4, B-9000 Ghent, Belgium

Received 12 October 2012, in final form 6 March 2013
Published 28 March 2013
Online at stacks.iop.org/PPCF/55/055001

Abstract
Sheaths tend to form when immersing metallic objects in plasmas. As it avoids the need to capture the sheath details, which occur on the Debye length scale while antennas are typically various orders of magnitude larger, the sheath boundary condition due to D'Ippolito and Myra (2006 *Phys. Plasmas* **13** 102508, 2008 *Phys. Plasmas* **15** 102501) offers antenna designers a major reduction in the numerical problem size they face. The sheath boundary condition was derived by making a number of simplifying assumptions to enable finding an analytical approximation of the conditions rapidly oscillating waves have to satisfy beyond the sheath that forms close to such objects. This paper discusses the solution of the cold plasma wave equation for sheath relevant density profiles, e.g. highlighting the role of the orientation of the static magnetic field and of oblique incidence, and underlining the impact the density profile has on the wave physics. It illustrates that the cross-talk between the waves impinging on and those excited at the wall and in the sheath sensitively depends on a number of parameters. The 2×2 connection coefficient matrix that is numerically obtained captures the sheath region fast time scale wave physics for a given density profile. When supplemented with a satisfactory model for the slow time scale variation it is a numerical tool that permits upgrading the realism of the fast time scale wave physics contained in the sheath boundary condition and that can help delimiting the range of applicability of simplified models, and assessing if a sufficiently general set of boundary conditions to describe the effect of the sheath can at all be constructed.

(Some figures may appear in colour only in the online journal)

1. Introduction

Due to the different mobility of ions and electrons, placing metallic objects in a plasma gives rise to highly localized sheaths (see, e.g., [1]) which repel the electrons and attract the ions. Since the voltage change in the sheath happens on a scale length of the order of the Debye length, the localized voltage change routinely gives rise to electrostatic fields strong enough to accelerate the ions. As such ions are natural candidates to cause hot spots and sputtering (see, e.g., [2, 3]), understanding how they are created and hopefully avoided is of importance for allowing long-term plasma operation in magnetic fusion machines. Ion cyclotron resonance heating (ICRH) antennas are metallic objects, commonly installed in a protecting metallic box with Faraday screen bars installed between the antenna straps and the main plasma. Because of the undesirable effects they cause, the formation of ICRH-induced sheaths has been extensively studied the last years (see, e.g., [4–15]). In spite of the fact that there is a finite density near the antennas (see, e.g., [7, 15]), the details of sheath physics are largely omitted when designing antennas. More often than not, and in spite of the very high level of sophistication of the geometrical details of the launchers that are accounted for (see, e.g., [16, 17]), even the very presence of a plasma in or near the antenna box is omitted altogether. There is an ongoing effort to refine the wave description needed to describe the near-field more accurately. Myra and D'Ippolito have been instrumental in pushing forward the level of sophistication with which sheaths are described; the majority of the earlier given references refers to their work. One of their major achievements in this respect is that they have formulated a 'sheath boundary condition' that allows

accounting for the effect of the sheath in a simplified way. In spite of the appeal of the approach they present (which amounts to replacing the two boundary conditions $\vec{E}_{\text{tangential}} = \vec{0}$ the rapidly varying electric field satisfies at the metallic walls by two other boundary conditions imposed beyond the narrow sheath, only a few Debye lengths away from the wall), the underlying physical model that describes the sheath is fairly crude: it assumes that the ions are nonresponsive and that a density gap is created in the sheath. The obvious advantage is that the solution of the Poisson equation can then be found by hand, and its solution can subsequently be used to formulate the new boundary condition. The damping in the sheath is modeled by adding an imaginary part to the vacuum dielectric constant $\epsilon = \epsilon_o \rightarrow \epsilon_o(1 + i\zeta)$. The actual shape of the density in the sheath is never computed and thus not accounted for, neither in the electrostatic description underlying the sheath physics nor in the fast time scale dynamics. Although clearly in the interest of keeping the formulation simple to allow easy implementation in numerical codes computing the antenna near-field, the obvious question poses if the proper density change should not be incorporated and if the wave dynamics implicitly contained in the sheath boundary condition is general enough to be meaningful. After all, it is the ion acceleration in the sheath that is thought to be responsible for sputtering and the formation of hot spots. The details of the charge separation and thus the ion and electron densities in the sheath are intimately connected to the (static) potential that accelerates the ions. Also on the fast time scale one can expect the waves to respond to the imposed density profile. Hence a model that assumes nonresponsive ions and infinitely mobile electrons is expected to have limitations when describing the waves close to a metallic object in a plasma in an attempt to shed light on sputtering and hot spot physics.

A simple, purely numerical study from first (known cold plasma) principles of the fast time scale wave physics is the subject of this paper. Its mere aim is a study of the wave physics close to metallic objects immersed in a plasma adopting a simplified model for the density variation in the sheath, revealing the importance of effects such as oblique incidence and the magnetic field direction on the coupling of the waves the plasma admits near metallic surfaces. This paper assumes the density profile is given. In a companion paper, the global density depletion in the antenna region while omitting the sheath effects was discussed [18], equally returning to the first principles to describe the effect. The description of the cross-talk between the two time scales is a large scale work that necessitates taking a step back from the usual cold plasma dielectric tensor description and incorporating flow terms in the description. It is outside the scope of this paper and will be discussed elsewhere.

The cold plasma wave equations are solved in the thin region close to a metallic object and a connection coefficient approach is presented which—once supplemented with a more general model for the density response resulting from the charge separation—could constitute the fast time scale wave part of a generalization of the sheath boundary condition method proposed by Myra and D'Ippolito to situations where the wave–plasma interaction modeling has been stepped up. Myra *et al* examined the connection coefficients treating the sheath as a vacuum layer rather than accounting for the actual density profile. In their model the presence of the plasma is accounted for by considering the proper dielectric response at the sheath–plasma interface [9]. Between plasma and vacuum, a discontinuous density jump is implicitly present. The density is assumed as given in the present computations, i.e. the impact of the fast time scale physics on the slow time scale physics is not yet studied. Rather than tackling the full problem at hand, an idea of the complexity of which is sketched in the next section, this paper merely illustrates the sensitivity of the waves to various parameters. It does so using the usual cold plasma description. *If* the physics in the sheath can be dominantly captured using a 1D model, the philosophy of the sheath boundary condition can likely be upgraded to include more physics. If that is not the case, the idea of adopting the sheath boundary condition to avoid needing to include it in antenna near-field computations has to be given up and a proper modeling of this region unavoidably becomes numerically challenging in view of the vastly different length scales that are of importance.

The text is structured as follows: in the next section, some preliminary notes are given on the subtleties of modeling the sheath density profile and what it takes to grasp the radio frequency (RF) sheath physics. In section 3, the cold plasma wave model is described. Section 4 is the heart of this paper: it discusses the wave dynamics in a cold plasma close to a metallic wall for a given density profile. Section 5 contains conclusions as well as a discussion on what needs to be carried out to ensure a more self-consistent description of the ICRF-induced sheaths. For the interested reader, a crude method for evaluating the charge neutrality violation near metallic objects immersed in a plasma and in the presence of a strong confining magnetic field in an arbitrary direction is provided in the appendix. This addition illustrates what an approximate density profile that can be used when solving the wave equation on the fast (ion cyclotron) time scale qualitatively looks like, justifying the simple parametrization used; the (Debye) scale length of the density variations it predicts is the main input for the fast time scale dynamics. At no point in the present text is the coupling of the fast and slow time scale problems addressed; on this point, the model due to Myra and D'Ippolito contains more physics than the model presented here. In the model for the slow time scale dynamics the back-coupling of the fast on the slow time scale is completely omitted.

2. Preliminary notes on the modeling of sheaths

Many authors have modeled sheaths highlighting various aspects relevant to sheath physics. The philosophy adopted in this paper which focuses on the fast time scale wave dynamics in the sheath is to assume the density profile to be used in the wave equation is known and given by the slow time scale dynamics. Except for a qualitative fluid-type model that describes the slow time scale dynamics and offers an idea of what the density profile looks like in the sheath, no effort is made to address the slow time scale problem, nor to model the cross-talk between the wave–plasma interactions on both

time scales. Moreover, also the usual cold plasma dielectric description will be adopted, in spite of its limitations. Rather than offering a full solution to the RF sheath problem, the mere goal of this paper is to demonstrate that capturing the wave dynamics and wave–wave interaction in the sheath close to a metallic wall necessitates accounting for the impact of various parameters on the waves and that more work is needed to ensure a more rigorous description.

When RF waves penetrate the sheath, capturing the interplay between the electrostatic potential and RF waves is of key importance. This is commonly carried out via the rectified potential Φ. The latter is related to the voltage difference $V_{\mathrm{RF}} = \int \mathrm{d}\vec{x}_{\parallel} \cdot \vec{E}$—measured along a magnetic field line and in which $\vec{E}$ is the RF electric field—through $\Phi = C|V_{\mathrm{RF}}|$. Adopting a 1D parallel plate capacitor model and integrating the ensuing sheath equations of the thin plasma between the plates numerically, Riyopoulus [19] and Myra [5] found a value for the factor C linking the fast and slow time scale wave dynamics; it typically takes values around 0.5. It is found that various parameters (e.g. the density, the orientation of the ion flow and that of the magnetic field) have a non-negligible impact on the results, details being sensitive to what happens in the first few Debye lengths away from the capacitor plates where charge neutrality is violated. In view of the sensitivity of the results, Riyopoulos notes in his conclusions that 'the development of a 2D sheath theory seems essential to further improve the description of magnetized sheaths' beyond the simplified model describing the sheath dynamics consistent with an imposed 1D voltage driven electric field $E = -\mathrm{d}V/\mathrm{d}x$ between 2 capacitor plates. Provided the sheath boundary condition faithfully describes the relation between the sheath voltage and the RF electric field, it allows one to extend the usual near-antenna-field modeling to include some key aspects of the impact of the sheath. Kohno adopts the sheath boundary condition to study the wave dynamics in the neighborhood of the antenna [20, 21]. Recently, D'Ippolito generalized the sheath boundary condition to include the effect of a fast wave impinging on the sheath, and involving both the reflected fast and slow waves in the updated condition. So far, to the authors' knowledge, the more general case of an arbitrary wave impinging on a sheath region with a density profile has not yet systematically been addressed. As Riyopoulos and Myra address the sheath dynamics (and reveal its sensitivity) omitting the details of the wave physics brought about by the plasma, one may wonder if such findings can indeed be applied to describe the dynamics in the whole antenna region—as opposed to the thin sheath region—in the presence of 3D electromagnetic fields that respond to and interact with the local density and magnetic field and are not just passively driven. An elegant solution that maximally builds on existing knowledge would be to generalize the sheath boundary condition as proposed by Myra and D'Ippolito [6, 8, 10–12] to account for the sheath physics and connect it to a 'non-sheath' model that accounts for the 3D evolution of both the slowly varying electrostatic $\vec{E}_{\mathrm{o}} = -\nabla\Phi$ responsible for zero order flows as well as the rapidly varying $\vec{E}_{(\mathrm{RF})}$ together with the relevant plasma parameters (density, flow velocity) away from the direct proximity of metallic objects. Colas *et al* [22] and Jacquot *et al* [14] made a first attempt in this direction by solving an equation for the slow time scale voltage and coupling it to the slow wave solution on the fast time scale; the fast wave is excluded in their description and the metallic walls are assumed to be electrically grounded. They point out how particularly challenging the problem of a proper modeling of the sheath is. Their more rigorous description of the slow time scale physics and the coupling of the 2 very different time scales is a worthwhile extension of the philosophy underlying Myra and D'Ippolito's work.

Since metallic walls both are bombarded by charged particles but equally allow currents to flow along—and penetrate in a thin layer under—their surface, the voltage to which they charge is not well known. Even if the metallic structures are grounded at some reference point, they need not instantaneously be at the same voltage at other places. Nevertheless solving the Poisson equation that describes the charge separation is often done assuming the voltage on the metallic surface in front of which the sheath forms is known. On top of that the plasma tends to interact with the wall in a number of ways, simply capturing electrons being the simplest.

Godyak developed a self-consistent dynamical model for RF sheaths with frequencies between the ion and electron plasma frequencies, be it in the absence of a confining magnetic field [23]. Godyak's results for floating dc potentials and for collisional and collisionless regimes converge to known limits in the high voltage approximation but for voltages of tens and hundreds of volts they disagree while being in good agreement with the experiment. Borrowing terminology from electronics, the ion acceleration-related wave damping in the sheath is written in terms of a (complex) impedance, containing a resistive and a capacitive contribution. For sufficiently small volumes, particle-in-cell (PIC) simulations have allowed one to grasp the sheath physics (see, e.g., [24, 25]): PIC simulations have successfully reproduced experimental findings [26] for argon capacitive RF discharges. In (all-metal) tokamak applications the relevant volumes are much larger. However, if the type of approach pioneered by Myra and D'Ippolito—or an extension of it—can be proven to be useful, PIC methods may be instrumental in helping to understand the RF induced sheaths.

In contrast, Stangeby addressed the sheath problem for the case where ICRH waves are absent but a confining magnetic field is present [27]. One aspect his work focuses on is the particular case when the magnetic field is almost grazing the metallic wall. As the particle motion parallel to a strong confining field is much more free that that in the perpendicular direction, while the dynamics normal to a metallic surface is characterized by scalelengths much shorter than that parallel to it, the limit of the confining field tilting to align with the wall is a limit that requires special attention. Apart from that, Stangeby addresses both the case where the wall is at a floating potential and the case where it is not.

Many authors impose an ion velocity at the interface of the sheath with the main plasma (where charge neutrality is restored) that is equal to or larger than the local sound velocity

('Bohm criterion'). Callen [1] demonstrates that an actual sheath is formed when the Bohm criterion is satisfied but equally shows that ion velocities can very well be smaller, in which a sheath does not form but an oscillatory rather than exponential behavior is observed close to the metallic wall instead. On the other hand, Zhang pointed out that ion streaming instabilities can occur in plasmas with multiple ion species [28], highlighting the fact that properly capturing the slow time scale dynamics is likely impossible when adopting very simple models that do not represent the interplay between particles with different charges and concentrations.

The necessity to have a flow at the sheath edge forces one to assume a finite velocity at the interface of the sheath with the main plasma. In kinetic models (see, e.g., [29–31]) such flow in one direction can be interpreted as the particles of a population having the proper sign of their velocity component normal to the wall. Such a modeling allows one to demonstrate that the Bohm criterion does not uniformly need to be satisfied in the sheath dynamics context but depends on the model adopted. Kinetic models also show that the sheath may not be limited to a few Debye lengths but may be substantially larger [29, 32], hinting at the possible need of a model that captures slow and time scale physics—and their cross-talk—in a wide region that not only includes the close vicinity of the metallic wall.

Another closer examination of the Bohm criterion was performed by Yankun [33]. This time, the fluid approximation is adopted but a finite (be it small) magnetic field is considered. It is shown that both the strength and orientation of the magnetic field affect the ion speed, and thus the density profile that is set up. The work of Yankun is a generalization of the expression proposed by D'Ippolito and Myra and reduces to it when the conductivity is zero.

If anything, a glance through the extensive amount of literature on the subject demonstrates that the actual density in the sheath strongly depends on a number of parameters. As the computation of the density itself is outside the scope of this paper, only a sketch of the type of density profiles and charge separation will be given in the appendix to provide the reader a justification for the type of profiles taken in the section discussing the (fast and slow, and incoming and outgoing) wave interaction due to the presence of the wall and of the density inhomogeneity and charge separation. As is already clear from the work of various authors mentioned above, the self-consistent determination of the ion and electron density variation between the wall and the main plasma requires iteratively solving the fast and slow time scale equations. As the potential in the sheath drastically changes the zero order slow time scale flow of the charged species and thus their density, the usual cold plasma dielectric tensor model—in which the nonlinear convective term $\vec{v}\cdot\nabla\vec{v}$ in the equation of motion has been omitted as it is assumed that there are no zero order flows $\vec{v}_o$ and that the perturbed flow is indeed merely perturbative so that the nonlinear term is small compared with the rapidly varying $\partial\vec{v}/\partial t = -i\omega\vec{v}$—is not adequate to describe the sheath, and possibly not even the whole antenna region. The simplest possible model allowing one to capture this cross-talk is the set of 14 equations (the vectorial Maxwell equations, the equation of motion and the continuity equation for electrons and ions) coupled on the two time scales and adopting a quasilinear approach to ensure the back-coupling from the fast to the slow time scale (a brief discussion of the philosophy is given in [18]); including an energy equation apart from the momentum equation further increases the number of equations to be solved simultaneously. Such a full discussion will require extensive progress and is not intended here.

Simple sheath models assume that ions are immobile while the electrons have a Boltzmann distribution, responding to the local potential to ensure the equation of motion is satisfied. In practice the ions cannot be immobile (otherwise sputtering and hot spots would not be an issue) and the electrons respond to the potential in a way that is not just responding to the potential arising from charge separation (i.e. including convection yields a density that is not just of the Boltzmann type but to a density that slightly deviates from it as the velocity, potential and density are coupled quantities). Whereas the electron velocity corrections are often small with respect to the electron thermal velocity, they are meaningful on the ion speed scale and tend to affect the current density which is composed of moving electrons and ions. In particular for ions, the fact that flow speeds of the order of the thermal velocity are created not only has an impact on the slow time scale but also on the fast time scale physics since it invalidates the zero flow assumption used to derive the usual cold plasma dielectric tensor. Devaux *et al* [32, 34] did a detailed study of the ion and electron density and found that the density is reduced when approaching the charged metallic wall. Similar profiles are found in other works (see, e.g., [35]). As the ions are less mobile than the electrons, they respond less readily to the potential and hence the electron density is more depleted than that of the ions. The various sheath density profiles the authors found in the literature are all of the same generic type. In the next section the sheath density will be parametrized as $N_\alpha = c_o + c_1\exp[-x/\lambda]$ with $c_o = N_{wall} - c_1$ and $c_1 = (N_{wall} - N_{plasma})/(1 - \exp[-x_{plasma}/\lambda])$ and a density $N_e = Z_i N_i$ at the sheath–plasma interface. The parameters λ as well as the fractions $N_{i,wall}/N_{i,plasma}$ and $N_{e,wall}/N_{i,wall}$ can then be used as independent parameters to assess the response of the waves to various characteristics of the density profile. The limit $\lambda = \infty$, $N_{i,wall}/N_{i,plasma} = 1$ and $N_{e,wall}/N_{i,wall} = 0$ is the case where the ion density does not budge while the electron density drops discontinuously to zero at the entrance of the sheath. This is the model adopted in the derivation of the sheath boundary condition of Myra and D'Ippolito.

3. Fast time scale response

Once the density modification due to the sheath is known, the (fast scale) wave equation can be solved. In this paper the wave description is kept as simple as possible, by relying on known expressions to describe the wave dynamics and keeping the geometry simple.

As the edge temperature is low, finite temperature effects are of little consequence in the wave model and the usual cold plasma model (see e.g. [36, 37]) seems crudely adequate. Although intended to shed light on wave excitation in

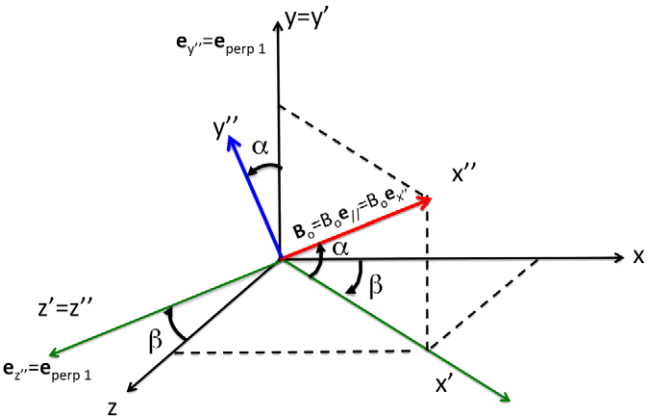

Figure 1. Sheath (x, y, z) and magnetic field (x'', y'', z'') based coordinate frames.

tokamaks, curvature effects are assumed non-essential hence a slab model is used. The magnetic field is assumed constant but has an arbitrary direction to represent any relative angle between the confining field and the local normal $(\vec{e}_x)$ to the metallic wall.

It is convenient to define two sets of Cartesian coordinates: the unit vectors $(\vec{e}_{\perp,1}, \vec{e}_{\perp,2}, \vec{e}_{\parallel})$ of the first form a right-handed set of perpendicular unit vectors in reference to the confining magnetic field. On the other hand, $(\vec{e}_x, \vec{e}_y, \vec{e}_z)$ is a right-handed frame in reference to the metallic wall immersed in the plasma, the coordinate x parametrizing the direction perpendicular to the wall. The two Cartesian coordinate frames $(x_{\perp,1}, x_{\perp,2}, x_{\parallel})$ and (x, y, z) are connected by two consecutive rotations (see figure 1). First keeping the y-axis fixed and then rotating around the new z-axis to lign up the final $x'' = x_{\parallel}$-axis with $\vec{B}$ yields

$$\begin{pmatrix} \vec{e}_{\parallel} \\ \vec{e}_{\perp,1} \\ \vec{e}_{\perp,2} \end{pmatrix} = \begin{pmatrix} \cos\alpha\cos\beta & \sin\alpha & \cos\alpha\sin\beta \\ -\sin\alpha\cos\beta & \cos\alpha & -\sin\alpha\sin\beta \\ -\sin\beta & 0 & \cos\beta \end{pmatrix} \cdot \begin{pmatrix} \vec{e}_x \\ \vec{e}_y \\ \vec{e}_z \end{pmatrix} = \overline{\overline{\mathcal{R}}} \cdot \begin{pmatrix} \vec{e}_x \\ \vec{e}_y \\ \vec{e}_z \end{pmatrix}. \quad (1)$$

Assuming the variations in the x-direction dominates the variation in the two independent directions tangent to the metallic wall, the y- and z-directions can be assumed to be ignorable and the variation of the rapidly varying electric field can be described by a double sum of decoupled Fourier modes (k_y, k_z). In terms of each (k_y, k_z) and eliminating the magnetic field, the wave equation can be written as

$$\left[\begin{pmatrix} k_y^2 + k_z^2 & 0 & 0 \\ 0 & k_z^2 & -k_y k_z \\ 0 & -k_y k_z & k_y^2 \end{pmatrix} + \begin{pmatrix} 0 & \mathrm{i}k_y & \mathrm{i}k_z \\ \mathrm{i}k_y & 0 & 0 \\ \mathrm{i}k_z & 0 & 0 \end{pmatrix} \frac{\mathrm{d}}{\mathrm{d}x} + \begin{pmatrix} 0 & 0 & 0 \\ 0 & -1 & 0 \\ 0 & 0 & -1 \end{pmatrix} \frac{\mathrm{d}^2}{\mathrm{d}x^2} \right] \begin{pmatrix} E_x \\ E_y \\ E_z \end{pmatrix} = k_0^2 \overline{\overline{\mathcal{R}}}^{-1} \cdot \overline{\overline{K}}_{\mathrm{NR}} \cdot \overline{\overline{\mathcal{R}}}$$

in which $\overline{\overline{K}}_{\mathrm{NR}}$ is the usual non-rotated cold plasma dielectric tensor with respect to the $\vec{B}_0$-based directions $(\vec{e}_{\perp,1}, \vec{e}_{\perp,2}, \vec{e}_{\parallel})$ [36]. In this paper, the accent is on discussing the sensitivity of the wave–wave interaction on the fast time scale and it will be assumed that the dominant dynamics is in the direction normal to the wall. If the y- and z-directions cannot be assumed ignorable, the problem becomes intrinsically multidimensional and the various (k_y, k_z) are coupled. In the former case the philosophy of adopting a sheath boundary condition beyond the sheath (rather than a metallic boundary condition at the wall) can possibly be upgraded adopting a suitable (1D) density profile while in the latter, a basically more general approach is needed. As E_x is a linear combination of the other two wave components and their first derivatives for each (k_y, k_z), it can be eliminated when solving the system. Note, however, that describing the variations along the magnetic field requires the differential operator

$$\vec{e}_{\parallel} \cdot \nabla = \cos\alpha\cos\beta\frac{\mathrm{d}}{\mathrm{d}x} + \mathrm{i}\sin\alpha\ k_y + \mathrm{i}\cos\alpha\sin\beta\ k_z,$$

i.e. that the parallel wave number is not a constant so that the dispersion equation cannot uniformly be evaluated in the usual way by first solving for a prescribed $k_{\parallel}$ to get the perpendicular wave numbers $k_{\perp}^2$, from which subsequently the k_x values can be found. Moreover, the dispersion equation generally is not a quadratic equation in k_x^2 but a quartic equation with both even and odd order terms in k_x which results in an asymmetry of the dynamics in the direction to and away from the metallic wall. Hence, the usual wave types (fast and slow waves) are present but the waves propagating toward the wall and away from the wall in general do not have the same wavelength.

Four boundary conditions are required to uniquely define the solutions of this fourth order differential equation. The boundary conditions at the metallic wall are $E_y = E_z = 0$. The other two boundary conditions are imposed at the interface x_{plasma} of the region of interest with the deeper plasma.

Assuming the wave power is efficiently absorbed inside the plasma, antenna modeling is commonly carried out imposing radiating boundary conditions, i.e. assuming that neither of the waves the plasma admits can carry energy into the antenna region from the plasma side. This assumption cannot be made for the present computation as we seek a way to substitute the two sheath boundary conditions proposed by Myra and D'Ippolito by a condition that allows one to account for the density actually imposed by the sheath physics, and expect waves to penetrate the region of interest and partially be reflected from it. Assuming the waves are decoupled at the plasma interface, the usual cold plasma dispersion equation—found by substituting $\mathrm{d}/\mathrm{d}x \rightarrow \mathrm{i}k_x$ in the above wave equation—can be solved and the four possible kinds of waves (two of the fast wave and two of the slow wave type) are identified. Solving the polarization equation for each of the wave types yields the eigenvectors. The independent variables and the eigenvectors are related by the matrix $\overline{\overline{T}}$:

$$\begin{pmatrix} E_y \\ \mathrm{d}E_y/\mathrm{d}x \\ E_z \\ \mathrm{d}E_z/\mathrm{d}x \end{pmatrix} = \overline{\overline{T}} \cdot \begin{pmatrix} s_{\mathrm{FW},\rightarrow} \\ s_{\mathrm{FW},\leftarrow} \\ s_{\mathrm{SW},\rightarrow} \\ s_{\mathrm{SW},\leftarrow} \end{pmatrix} = \begin{pmatrix} 1 & 1 & \cdots \\ \mathrm{i}k_{\mathrm{FW},\rightarrow} & \mathrm{i}k_{\mathrm{FW},\leftarrow} & \cdots \\ E_z/E_y|_{\mathrm{FW},\rightarrow} & E_z/E_y|_{\mathrm{FW},\leftarrow} & \cdots \\ \mathrm{i}k_{\mathrm{FW},\rightarrow}E_z/E_y|_{\mathrm{FW},\rightarrow} & \mathrm{i}k_{\mathrm{FW},\leftarrow}E_z/E_y|_{FW,\leftarrow} & \cdots \end{pmatrix} \begin{pmatrix} s_{\mathrm{FW},\rightarrow} \\ s_{\mathrm{FW},\leftarrow} \\ s_{\mathrm{SW},\rightarrow} \\ s_{\mathrm{SW},\leftarrow} \end{pmatrix}$$

and hence imposing the fast or slow wave to carry energy into the interval amounts to imposing the conditions $s_{\mathrm{FW},\rightarrow} \neq 0$ and $s_{\mathrm{SW},\rightarrow} = 0$ or $s_{\mathrm{FW},\rightarrow} = 0$ and $s_{\mathrm{SW},\rightarrow} \neq 0$ relating the independent electric field components and their derivatives through 2 linear relations. Although the solutions are expressed in terms of eigenvectors in this paper to make the interpretation of the wave cross-talk more intuitive, the waves do not need to be decoupled (satisfying the WKB criterion) at x_{plasma} for the proposed method to yield meaningful results.

The sheath boundary condition formulated by D'Ippolito and Myra provides two boundary conditions that can be imposed beyond the sheath so that the sheet dynamics does not need to be taken into account. Solving the above set of equations for the density profile found from a sheath computation allows one to add supplementary dynamics beyond the simplified, analytical description proposed by these authors. Solving the wave equation either assuming pure fast wave incidence or slow wave incidence on the sheath layer yields the complex connection coefficients that relate the eigenvector amplitude of the incoming and outgoing waves for both kinds of excitation. Alternatively, solving the equations for pure outgoing wave power on either of the modes yields the same connection matrix. The four obtained constants in this matrix constitute a generalization of the two sheath boundary conditions in a form similar to the surface impedance matrix often used in antenna modelling (see, e.g., [38]): to be consistent with the proximity of the wall and the density profile, the incoming and outgoing wave amplitudes are related by two conditions each of which prescribes what the outgoing wave amplitudes are for each of the two types of incoming wave amplitudes:

$$\begin{pmatrix} \vec{s}_{\mathrm{FW}\rightarrow} \\ \vec{s}_{\mathrm{SW}\rightarrow} \end{pmatrix} = \begin{pmatrix} C_{\mathrm{FW}\rightarrow,\mathrm{FW}\leftarrow} & C_{\mathrm{FW}\rightarrow,\mathrm{SW}\leftarrow} \\ C_{\mathrm{SW}\rightarrow,\mathrm{FW}\leftarrow} & C_{\mathrm{SW}\rightarrow,\mathrm{SW}\leftarrow} \end{pmatrix} \cdot \begin{pmatrix} \vec{s}_{\mathrm{FW}\leftarrow} \\ \vec{s}_{\mathrm{SW}\leftarrow} \end{pmatrix}.$$

In this paper, the eigenvectors were used to illustrate the cross-talk between the waves types via the sheath and the metallic boundary conditions clearly. Connection coefficients need not be formulated for this particular set of four independent variables. Any other choice—e.g. simply the original set $(E_y, \mathrm{d}E_y/\mathrm{d}x, E_z, \mathrm{d}E_z/\mathrm{d}x)$—is equally justified, and avoids the need of evaluating the dispersion roots.

In case local grid refinement schemes allow one to zoom-in in regions where it is required, the coupled fast–slow time scale problem may be tackled in a single go with the computation of the antenna near-fields in and near the antenna box. An attempt along these lines is the work of Jacquot *et al* [14] and Colas *et al* [22]. If that is not possible then the here suggested connection coefficient approach may (for a local decomposition of the field) allow one to define a generalized sheath boundary condition: any function of 1 (or multiple spatial) variable(s) can be written in terms of its (multiple) Fourier integral(s). A discrete version of this integral is often used to match 2 or 3D functions across interfaces so that the interfacing of the electromagnetic field between two different regions can be carried out per set of modes via a connection matrix; for an example in the ICRH antenna modeling, see [39] interfacing the fields inside the antenna box with fields in the core plasma relying on the surface impedance matrix. In this latter way, the need to look at the wave dynamics on the Debye length scale when computing the antenna near-field in larger volumes is avoided, which has clear computational advantages.

4. Examples of ICRF wave dynamics in the presence of a metallic object

This section concentrates on discussing the wave dynamics on the ICRF time scale. Here the (on the fast time scale) static density profile is used as a given input and represents the simplest possible upgrade of the 'vacuum gap' approach underlying the simplified dielectric model used in the derivation of the sheath boundary condition. Strictly, the net effect of the dynamics on the fast time scale when averaged over all fast time scale dependence is likely to modify the static density profile, and should be included in the description of how the density is set up. Such a treatment is more ambitious than the sensitivity analysis which is the more modest goal of this text. A single density profile (that for $N_{\mathrm{e}} = Z_{\mathrm{i}} N_{\mathrm{i}} = 10^{16}\,\mathrm{m}^{-3}$ and $T_{\mathrm{e}} = T_{\mathrm{i}} = 15\,\mathrm{eV}$) obtained in the appendix will be used to find the solution of the fast time scale wave dynamics. A D plasma to which a small minority of H has been added will be considered. Unless specified otherwise, the parameters are $f = 51\,\mathrm{MHz}$, $k_y = 2/m$, $k_z = 6/m$, $B_{\mathrm{o}} = 3.45\,\mathrm{T}$, $\alpha = 0.1\,\mathrm{rad}$, $\beta = 1.3\,\mathrm{rad}$ and $X[\mathrm{H}] = N_{\mathrm{H}}/N_{\mathrm{i,tot}} = 0.05$, parameters loosely inspired on the H minority heating scheme in JET. A small collision frequency $\nu = 10^{-2}\,\mathrm{Hz}$ was introduced to allow easy verification of causality. The integration of the wave equation is carried out using a finite difference procedure using 1000 points in the integration region.

The cold plasma supports two wave types, the fast and the slow waves. While the former has its main electric field component perpendicular to the static magnetic field and a parallel electric field component that is small, the latter's parallel electric field component is essential. Also the wavelength of the two waves is different, except in extremely low-density plasmas where the dispersion roots of both waves approach the same vacuum limit $k^2 = k_{\mathrm{o}}^2$. In spite of the density being high or low, the two waves can be identified through their polarizations (TE wrt the magnetic field for the former and TM for the latter).

The sheath boundary condition due to Myra and D'Ippolito implicitly assumes that the sheath density is so low that the dielectric response is well approximated by the vacuum permittivity. In view of the small width of the sheath, the solutions of the wave equation can then be found by hand and the fast and slow waves (almost) reduce to the vacuum transverse electric and transverse magnetic solutions of the vacuum wave equation. Figure 2 shows solutions of the wave equation for fast wave incidence when the density is of the parametric form described in section 2, with a plasma density $10^{17}\,\mathrm{m}^{-3}$, $N_{\mathrm{wall}}/N_{\mathrm{plasma}} = 0.7$, $N_{\mathrm{e,wall}}/N_{\mathrm{i,wall}} = 0.1$ and $\lambda = 0.001\,\mathrm{m}$. The angles of the magnetic field are chosen such that the metallic surface of interest is parallel to the last closed flux surface ($\beta = \pi/2\,\mathrm{rad}$); the finite $\alpha = 0.1\,\mathrm{rad}$ represents the angle between the toroidal and the parallel directions. Because of the limited extent of the sheath and

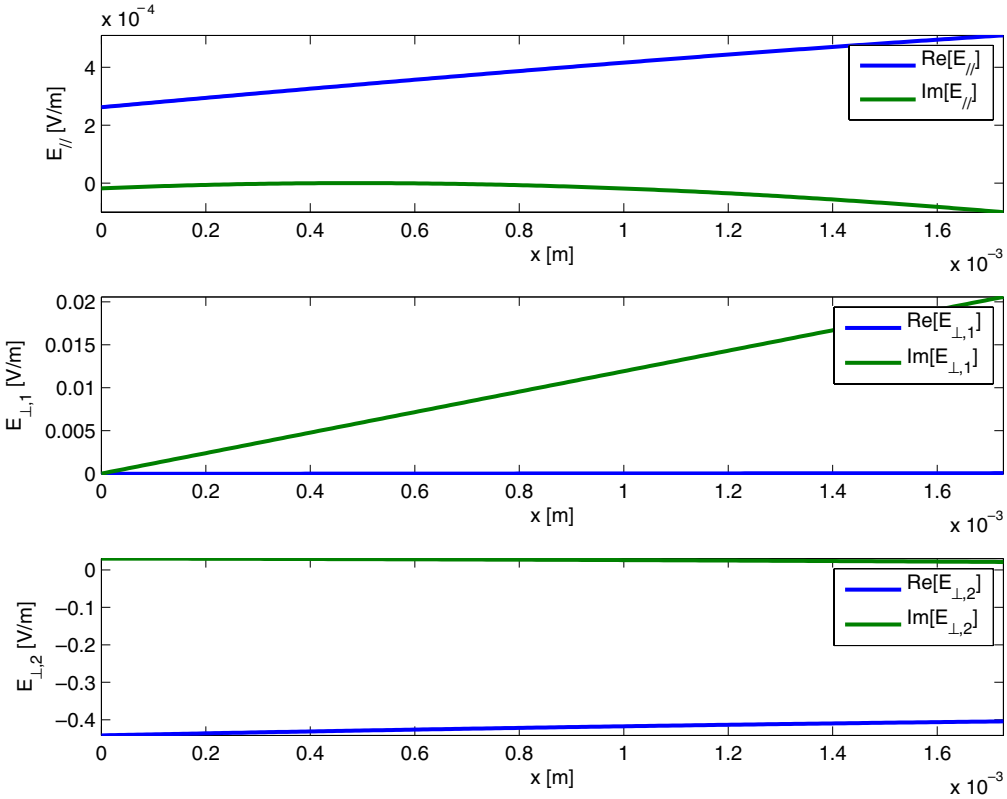

Figure 2. Electric field components for fast wave incidence and a plasma density of $10^{17}\,\mathrm{m}^{-3}$; $\alpha = 0.1$ rad, $\beta = \pi/2$ rad, $N_{\mathrm{wall}}/N_{\mathrm{plasma}} = 0.7$, $N_{\mathrm{e,wall}}/N_{\mathrm{i,wall}} = 0.1$ and $\lambda = 0.001$ m.

when the subregion of the sheath in which the slow wave is propagative is small, the various electric field components are essentially straight lines. Characteristic for the fast wave, the perpendicular components dominate the solution.

The slow wave is evanescent at high density but becomes propagative when the lower hybrid resonance is crossed. Figure 3 demonstrates its characteristic behavior. The plot on the left is for a plasma density of $10^{19}\,\mathrm{m}^{-3}$ while that on the right is for $10^{14}\,\mathrm{m}^{-3}$. Since both the fast and slow waves carry their energy electromagnetically (i.e. via the Poynting flux) the amplitude of a slow wave carrying the same energy as a fast wave typically has a smaller amplitude. Whereas the long wavelength component is usually dominating the electric field, the short wavelength component shows up more clearly in the field derivative and thus in the flux. Figure 4 shows both the field components and their derivatives for a case of slow wave incidence on the sheath and for a plasma density of $10^{18}\,\mathrm{m}^{-3}$. Whether or not the behavior of the waves in the sheath is similar to that in vacuum largely depends on the exact shape of the density profile, which determines where the fast and slow waves are propagative and where they become evanescent.

Behind the last closed flux surface—at which the density is still significant, especially when operating in H-mode—the density decays rapidly and hence it can be several orders of magnitude different depending on where exactly the wave dynamics is looked at. The importance of the density is demonstrated in figure 5. The $\log_{10}$ of the density at the plasma–sheath interface is used as an independent variable. The left figure shows the dispersion equation roots at the wall (each type of wave mode has a specific color and symbol), and the right figure shows the corresponding connection coefficients (following the same color coding for the wave mode imposed at x_{plasma} via the boundary condition, and the same symbols to represent the excited waves) referring to unit amplitude eigenvectors of each of the four possible types. At the wall, the slow wave dispersion equation root becomes evanescent at low density ($\log_{10} N_{\mathrm{e}} \approx 14.7$) where it ultimately joins the vacuum root. One of the slow wave roots goes through the lower hybrid resonance at $\log_{10} \approx 15.9$ (recall that $\partial/\partial x_{\parallel}$ is a differential operator and not just a constant $\mathrm{i}k_{\parallel}$, hence the wave behavior is not left–right symmetric). At any density, the fast and slow waves interact but the fast wave relies more on the existence of the slow wave than does the slow wave on the fast wave: to be able to satisfy the oblique incidence metallic boundary condition, longer wavelength modes need to excite short wavelength modes of more significant amplitude while the amplitude of the fast wave excited by the slow wave is very small. At the very density end of the plot, the dielectric tensor is essentially reduced to that in vacuum and—except for the fact that they characterize a transverse electric and a transverse magnetic wave with respect to the direction in which the confining magnetic field points, they now share the same dispersion and have the same wave character. Not surprisingly, the connection coefficients overlap in this density range. The differences between the modes only start appearing when at sufficient density the magnetic field plays its role of making the parallel and perpendicular dielectric response different on account of the different ion and electron mass.

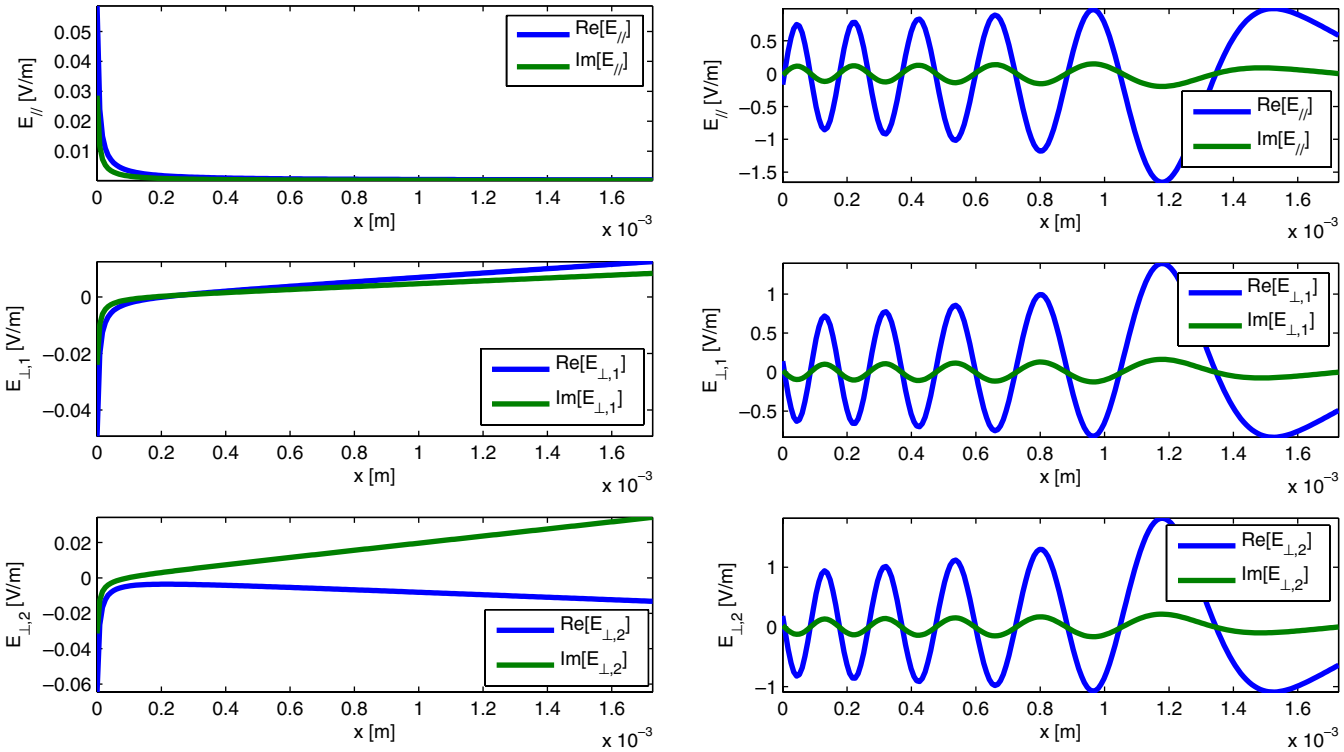

Figure 3. Electric field components normal to the metallic wall for slow wave incidence and a plasma density of 10^{19} m^{-3} (left) or 10^{14} m^{-3} (right); $\alpha = \beta = 0.7$ rad, $N_{\rm wall}/N_{\rm plasma} = 0.7$, $N_{\rm e,wall}/N_{\rm i,wall} = 0.01$ and $\lambda = 0.001$ m.

In a plasma of sufficient density, the fast wave and the slow wave respond differently to the presence of a strong magnetic field. D'Ippolito and Myra already pointed out the sensitivity of the coupling between the two waves to the orientation of the magnetic field [9] in their sheath boundary condition model. Figure 6 reveals that the direction of the magnetic field critically determines the cross-talk between the fast and the slow waves. For the chosen parameters, the fast wave is evanescent for any value of β but the slow wave both has β-regions where it is propagative and is evanescent. The lower hybrid resonance is crossed at two values of β. A unit amplitude incoming fast wave (red dashed–dotted lines in the connection coefficient plot) gives rise to a reflected fast wave with an amplitude slightly smaller than 1, and to an outgoing slow wave with an amplitude that is non-negligible for many values of β. Aside from a mode of the same character, the slow wave also necessitates a fast wave. Note that at the angles at which the hybrid resonance is crossed the connection coefficient to the other slow wave jumps discontinuously as well. At the angle where the wave switches from propagative to evanescent the connection coefficients cross the value 1.

As discussed in the previous section there is no need to evaluate all four independent solutions at the plasma side to fully determine the complex connection coefficients. The complex connection coefficient matrix relating ingoing to outgoing waves is just the inverse of the matrix relating outgoing to incoming waves and only the solutions consistent with either the two incoming wave types (lines 1,2 and 5,6 in the connection coefficient plot) or the two outgoing wave types (lines 3,4 and 7,8 in that plot) need to be evaluated. At $x = x_{\rm plasma}$, the electric field is a linear combination of the four independent solutions. The four independent connection coefficients prescribe the outgoing fast and slow wave amplitudes for an incoming fast wave or for an incoming slow wave. These two conditions avoid needing to evaluate the wave equation in the sheath region and replace it by two conditions to be satisfied beyond the sheath.

Figure 7 illustrates the simultaneous existence of fast and slow waves for a range of k_y values, i.e. for waves impinging obliquely on the metallic surface. As for the density, the exact value of the imposed wave vector component critically determines the importance of the cross-talk between the waves. Note (i) that the cross-talk in the region $k_y \approx 0$ is rather different from that where $k_y \gg 1$ (demonstrating that oblique incidence effects should be incorporated in a sheath model), and (ii) that the orientation of the magnetic field creates a breaking of the symmetry of the left and right propagating roots, and results in a breaking of the symmetry of the connection coefficients. Whereas D'Ippolito *et al* were aware of this sensitivity [9], figure 7 provides the results for a prescribed density profile.

In this paper the density profile is adopted as an input parameter. As the slow time scale dynamics determines its actual shape, modeling the coupling of the fast and slow time scale dynamics is required to find the self-consistent profile. Depending on what happens exactly on the slow time scale the density profile will qualitatively be the same but will differ quantitatively; an approximate model is provided in the appendix but more refined modeling is required to account for the subtleties of the density modification due to the

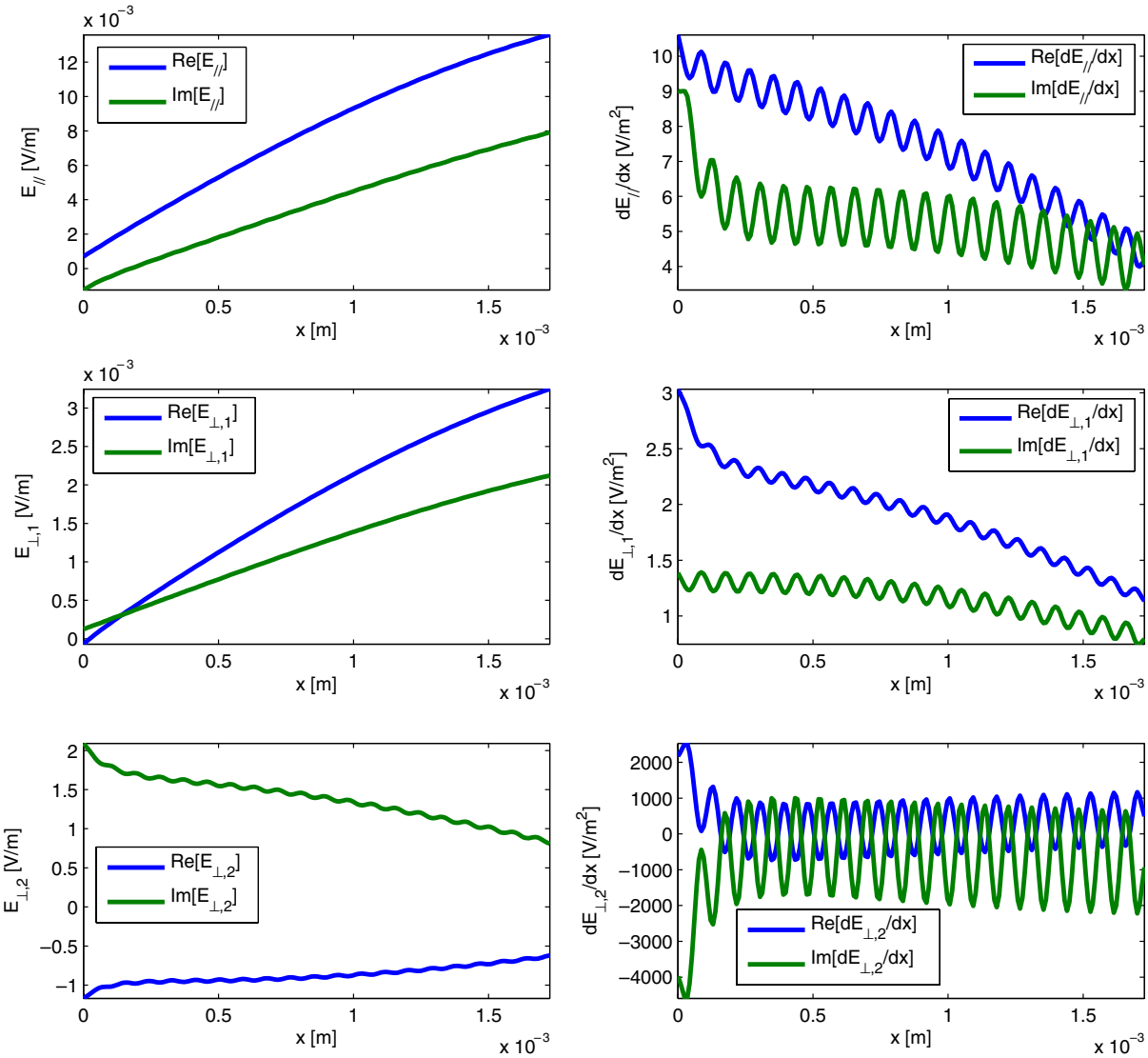

Figure 4. Electric field components (left) and their derivatives normal to the metallic wall (right) for slow incidence and a plasma density of 10^{18} m^{-3} ; $\alpha = 0.1$ rad, $\beta = \pi/2$ rad, $N_{\text{wall}}/N_{\text{plasma}} = 0.7$, $N_{\text{e,wall}}/N_{\text{i,wall}} = 0.01$ and $\lambda = 0.0001$ m.

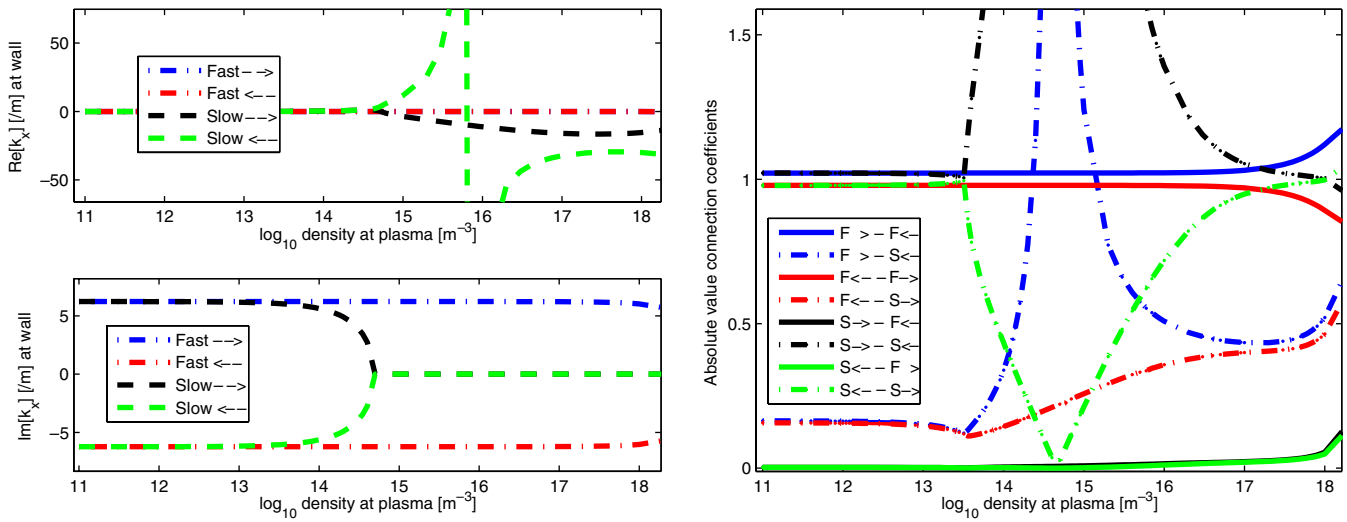

Figure 5. Dispersion roots and absolute values of the complex connection coefficients for unit amplitude eigenvectors for various plasma densities; the other density parameters are $N_{\text{wall}}/N_{\text{plasma}} = 0.7$, $N_{\text{e,wall}}/N_{\text{i,wall}} = 0.1$ and $\lambda = 0.001$ m.

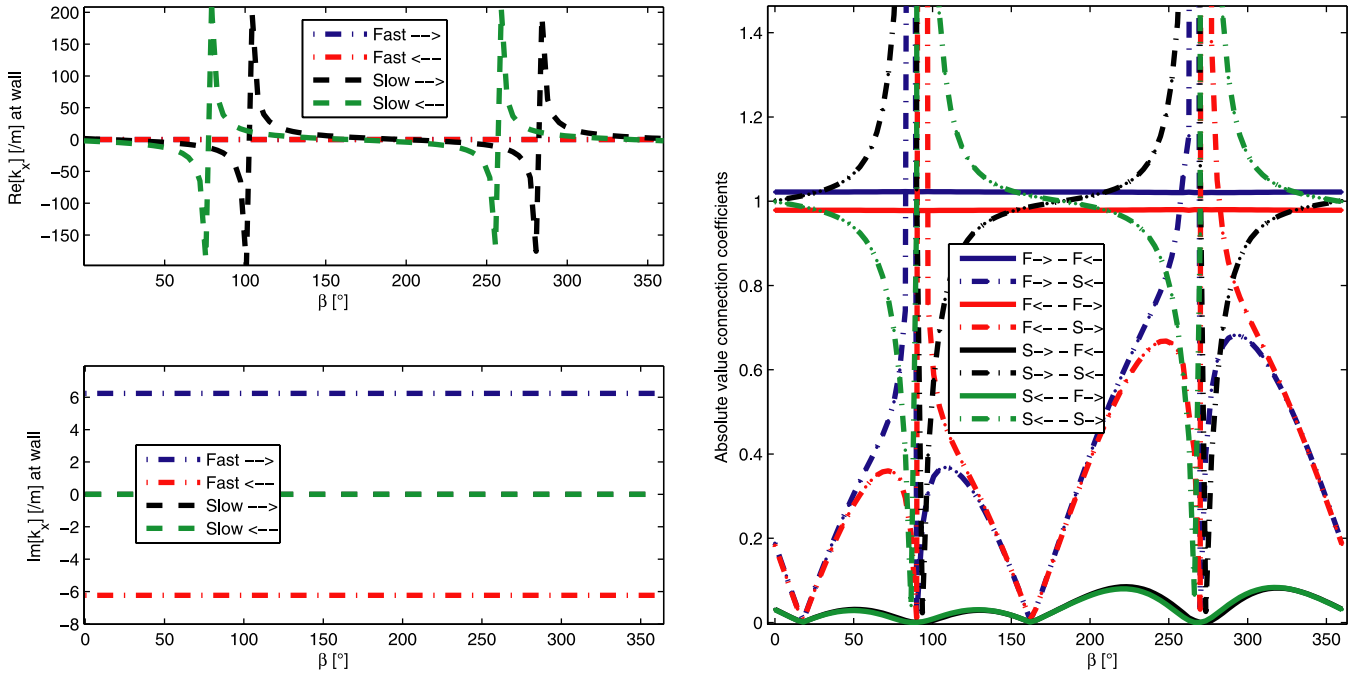

Figure 6. Dispersion roots and absolute values of the complex connection coefficients for unit amplitude eigenvectors for various β; the input density has parameters $N_{\mathrm{wall}}/N_{\mathrm{plasma}} = 0.7$, $N_{\mathrm{e,wall}}/N_{\mathrm{i,wall}} = 0.1$ and $\lambda = 0.001$ m.

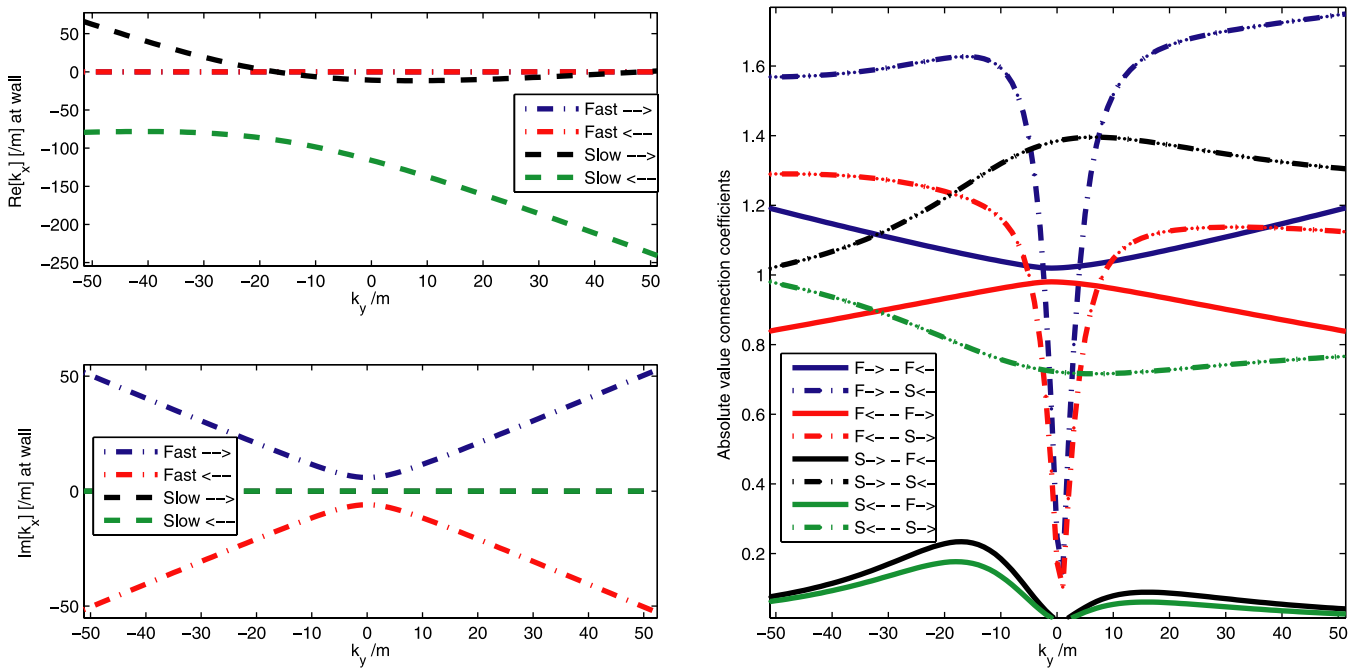

Figure 7. Dispersion roots at the wall and absolute values of the complex connection coefficients for unit amplitude eigenvectors for various k_y; the input density has parameters $N_{\mathrm{wall}}/N_{\mathrm{plasma}} = 0.7$, $N_{\mathrm{e,wall}}/N_{\mathrm{i,wall}} = 0.1$ and $\lambda = 0.001$ m.

waves. The sheath density can qualitatively be parametrized as $N_\alpha = c_0 + c_1 \exp[-x/\lambda]$ with $c_0 = N_{\mathrm{wall}} - c_1$ and $c_1 = (N_{\mathrm{wall}} - N_{\mathrm{plasma}})/(1 - \exp[-x_{\mathrm{plasma}}/\lambda])$. In the following figures, the density $N_{\mathrm{e}} = Z_{\mathrm{i}} N_{\mathrm{i}}$ at the sheath–plasma interface, the parameter λ as well as the fractions $N_{\mathrm{i,wall}}/N_{\mathrm{i,plasma}}$ and $N_{\mathrm{e,wall}}/N_{\mathrm{i,wall}}$ will be used to assess the response of the waves to the various parameters controlling the density profile.

Figure 8 depicts how the dispersion equation roots and the connection coefficients vary for a fixed plasma electron density $N_{\mathrm{e,plasma}} = 10^{15}\,\mathrm{m}^{-3}$, $\lambda = 0.001$ m and wall electron-to-ion fraction $N_{\mathrm{e}}/N_{\mathrm{i}} = 0.2$ at the wall but scanning the fraction of the ion density at the wall compared with that at the interface of the sheath with actual plasma. The other parameters are kept constant. The dispersion roots are depicted at the plasma wall (for the present scan, they do not vary at the plasma interface). The slow wave is propagative in the high density region but becomes evanescent for $N_{\mathrm{wall}}/N_{\mathrm{plasma}} \approx 0.18$. For different $N_{\mathrm{wall}}/N_{\mathrm{plasma}}$ the

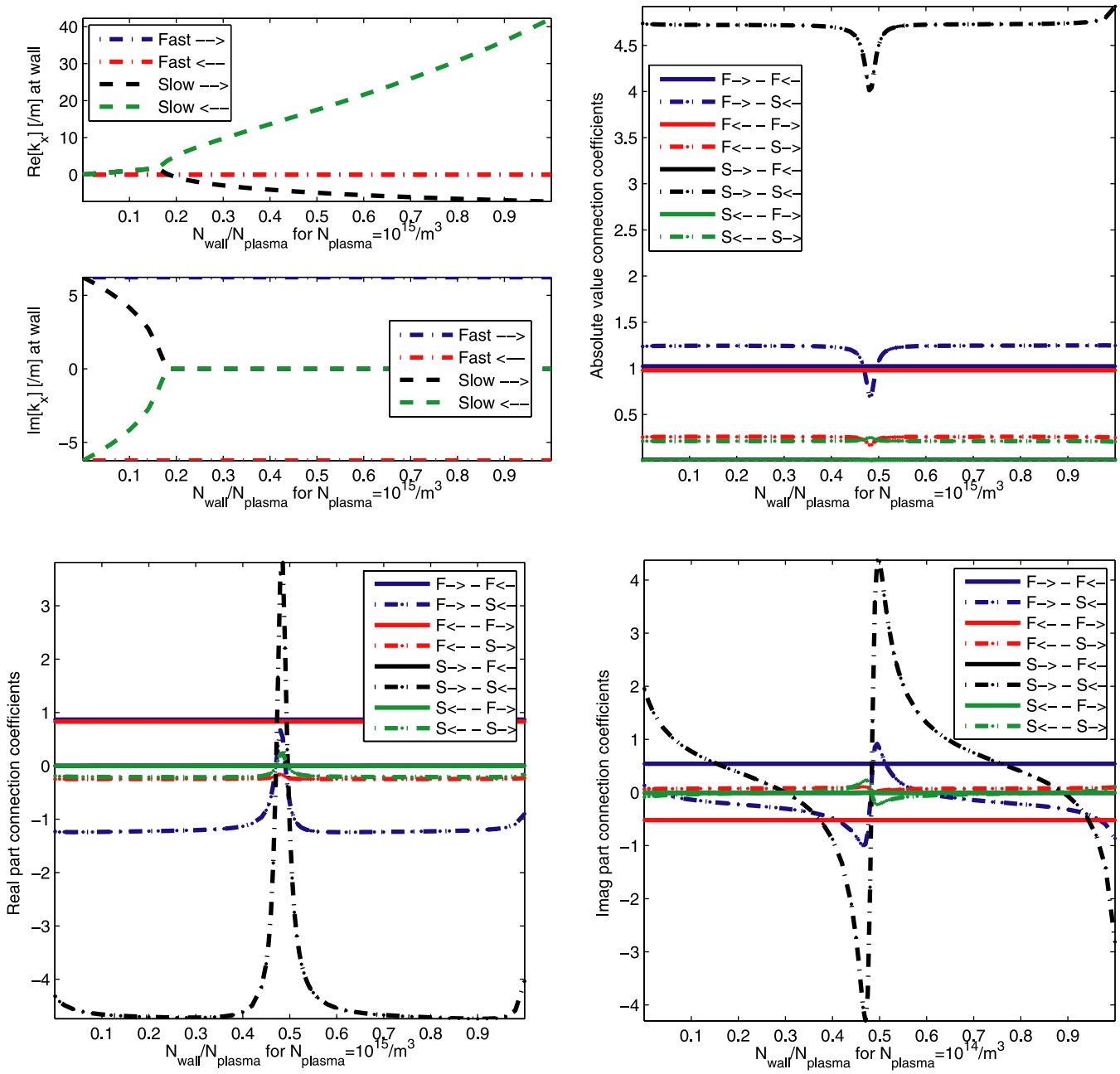

Figure 8. Dispersion roots at the wall (top left), absolute values (top right), real parts (bottom left) and imaginary parts (bottom right) of the complex connection coefficients for unit amplitude eigenvectors for various wall-to-plasma ion density fractions and for a plasma density of $10^{15}\,\mathrm{m}^{-3}$, $N_{\mathrm{e,wall}}/N_{\mathrm{i,wall}} = 0.2$ and $\lambda = 0.001\,\mathrm{m}$.

density changes everywhere inside the plasma, which, e.g., displaces the positions of where exactly in the plasma the waves go from propagative to evanescent behavior. Globally, this seems to be of little importance but at $N_{\mathrm{wall}}/N_{\mathrm{plasma}} \approx 0.48$ there is a different interaction between fast and slow waves. To the exception of that parameter region and for the chosen set of parameters, figure 8 mainly demonstrates that although the dispersion and thus the wave character changes, the absolute value of the connection coefficients do not change much. This seeming lack of sensitivity to the density is somewhat deceiving, however, as the bottom plots demonstrate: although the amplitude of the excited modes is identical for different densities at the wall, there is a gradual phase shift that is significant. Models that do not account for the actual density profile cannot capture this density-related phase shift.

The same is true when scanning the electron-to-ion density at the wall, as shown in figure 9, freezing $N_{\mathrm{wall}}/N_{\mathrm{plasma}}$ to 0.6. Again the dispersion is plotted only at the wall position. In this case the impact of the lower hybrid resonance can clearly be observed on the dispersion roots evaluated at the wall when $N_{\mathrm{e}}/N_{\mathrm{i}} \approx 0.75$, but it is present at other densities away from the wall. At the wall, the slow wave becomes evanescent at $N_{\mathrm{e}}/N_{\mathrm{i}} \approx 0.06$. The interplay of the cutoffs and resonances of the waves locally cause deviations of the connection coefficients, already clearly noticeable on the absolute value of the coefficients but much more clearly visible

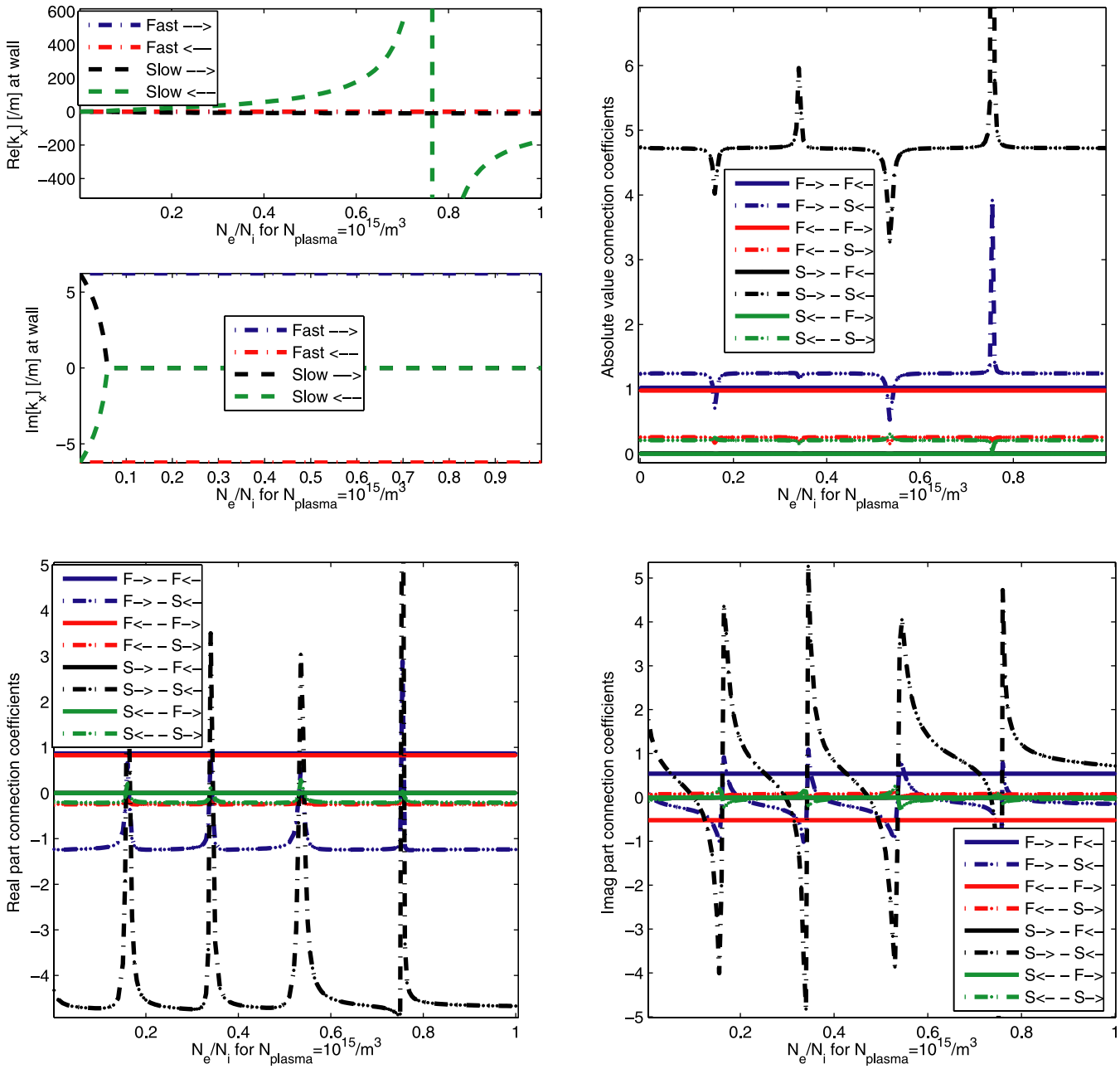

Figure 9. Dispersion roots at the wall (top left), absolute values (top right), real parts (bottom left) and imaginary parts (bottom right) of the complex connection coefficients for unit amplitude eigenvectors for various wall electron-to-ion fractions for a plasma density of 10^{15} m^{-3}; $N_{\text{wall}}/N_{\text{plasma}} = 0.6$ and $\lambda = 0.001$ m.

on the coefficients' real and imaginary parts. The propagative nature of the slow wave, and its impact on the coupling of the waves, requires accounting for the density profile. Note that the fast and slow waves' connection coefficients differ quantitatively. A slow wave entering the sheath region ($|\vec{s}_{S,\leftarrow}| = 1$; $|\vec{s}_{F,\leftarrow}| = 0$) hardly gives rise to the excitation of an outgoing fast wave and also has a significantly reduced amplitude slow wave exciting. As both fast and slow waves carry energy via the Poynting flux, one can readily conclude when looking at the dispersion plot that the slow wave's amplitude reduction is a consequence of the fact that $|k_x|$ is much larger for the outgoing than for the incoming slow wave, the difference being a direct consequence of the fact that the parallel wave number is not constant because the confining magnetic field has a nonzero component in the x-direction. On the other hand, an incoming fast wave produces an outgoing fast wave of almost the same amplitude and an outgoing slow wave of which the amplitude is not negligible either.

A scan of the parameter λ yields similar results. Not surprisingly the overall density level is the most important of the various parameters that determine the density profile.

5. Discussion and future work

This work demonstrates that the ICRH dynamics in the sheath close to metallic objects in plasmas is rich and

requires accounting for effects such as the wall orientation wrt the confining magnetic field and the actual density profile in the sheath, the latter being a sensitive function of the sheath characteristics (voltage to which the wall loads up, temperature, zero order parallel velocity, potential, etc). Although the fast varying fields are most sensitive to the variations perpendicular to the metallic wall when close to the wall, the variations parallel to the wall play a non-negligible role as well. It was, e.g., shown that the wave couplings for perpendicular incidence and oblique incidence are qualitatively different. Whereas a model that treats the sheath layer as a vacuum zone allows one to solve the wave equation by hand, as Myra and D'Ippolito have demonstrated in their work, it lacks the possibility to account for the impact of the location of cutoffs and resonances. Solving the wave equation in the sheath region numerically, it was shown in this paper that the actual density profile often has a non-negligible impact on the interaction between the waves. In view of the relative insensitivity on density in specific density intervals (when no cutoffs or resonances occur in the sheath), the original sheath boundary condition should yield connection coefficients that are broadly trustworthy.

One important aspect addressed in the sheath boundary condition by Myra and D'Ippolito has not been touched upon here: in response to the fast electric field, the sheath itself varies. Consequently an iterative process needs to be set up to account for the back-reaction of the fast time scale effects on the slow time scale physics. Antenna modelers do this using the sheath boundary condition in an iterative way, solving the wave equation until a self-consistent stage has been reached. Whereas this is fairly straightforward for the simplified sheath description, it becomes less trivial when the dynamics is more rigorously included: as demonstrated in the given examples, the generalized sheath boundary condition yields different results for different densities, static magnetic field orientation, wave scale length in the ignorable directions, etc. Hence, these effects need to be included in a sheath boundary condition that accounts for the rich wave dynamics in the sheath in a more satisfying way. This clearly is not straightforward as it significantly increases the level of sophistication contained in the boundary condition. An alternative—seemingly more simple and natural—approach following the here adopted logic of including the sheath effect by solving the wave equation using the actual density profile found from a separate charge separation computation is to solve the cold plasma equations in the whole (antenna) region of interest—and not just the sheath region, as is done here—relying on grid refinement techniques. Efforts in that direction prove promising (see the work by Crombé [40]), although it is not at all clear if the memory requirements are not prohibitive for the complicated geometries of actual antennae; moreover, not only in the sheath region but in the whole near-field region do the RF waves modify the density profile (see [18]).

Since the net effect of the fast time scale is to trigger density variations and drift velocities, the here adopted 'standard' cold plasma description (which assumes zero order drifts are absent) is not adequate for capturing the full physics of the wave-plasma cross-talk and hence the usual cold plasma dielectric formulation needs to be upgraded if a truly self-consistent description is aimed at. This requires going back to first principles and simultaneously solving Maxwell equations together with the equation of motion and the continuity equation (possibly augmented with the energy equation) rather than solving the equation of motion is an approximate way, as is carried out to formulate the cold plasma dielectric tensor. Although this may sound straightforward, it is a major numerical challenge that awaits to be initiated: It requires (i) developing a model that accurately describes the interaction of the density, velocity and electromagnetic field variations driven at high frequency ω and for a given density flow and electrostatic field, (ii) developing a similar model that accurately describes the slow dynamics for a given set of quasilinear terms consistent with a given RF perturbation, and (iii) coupling the two models. Excluding an explicit equation for the energy evolution and assuming that there are only two types of species—electrons and one type of ions—this yields a system of 14 coupled equation on each of the two time scales. Assuming the perturbations are sufficiently small, the nonlinear terms can be omitted in the fast time scale equations and their time-averaged contributions can be included as essential corrections in the slow time scale equation. In the latter there is no justification for dropping or removing the nonlinear terms.

Appendix: A simple, qualitative model for the slow time scale plasma response

The plasma–wave interaction occurs on two vastly different time scales. Compared with the fast time scale, the slow dynamics can be considered time-independent. In this appendix, the latter dynamics is discussed using a model meant to sketch why various quantities play a role but that otherwise is kept as simple as possible. To describe the response of the plasma to the presence of metallic objects and the charge separation that will result from it because of the different mass-dependent ion and electron mobilities, the wave equation needs to be solved in conjunction with the continuity equation for all plasma constituents. If a static equilibrium is reached, the charge separation gives rise to a static electric field that is consistent with the charge separation. The static electric field derives from a potential ($\vec{E} = -\nabla\Phi$) and the relevant wave equation is the Poisson equation,

$$\Delta\Phi = \frac{e}{\epsilon_o}\left[N_e - \sum_i Z_i N_i\right]$$

in which Φ is the field potential, e is the elementary charge, ϵ_o is the vacuum permittivity, Z_i is the atomic number and the sum is on the various ion species. Furthermore, N_α is the density of the (electron or ion) species of kind α. For each of the species types considered the dynamics is reigned by the equation of motion of a species 'fluid'

$$N_\alpha m_\alpha \frac{\mathrm{d}}{\mathrm{d}t}\vec{v} = -\nabla P_\alpha + N_\alpha m_\alpha \Omega_\alpha \vec{v} \times \vec{e}_\parallel - q_\alpha N_\alpha \nabla\Phi$$

(in which Ω_α is the cyclotron frequency and m_α is the mass) and the related continuity equation

$$\frac{\partial}{\partial t}N_\alpha + \nabla\cdot\vec{v}_\alpha N_\alpha = 0,$$

where the subscripts will henceforth be dropped when no ambiguity is possible; friction terms have been omitted and it will be assumed that the temperature appearing in the pressure term $P = NkT$ is constant. The last two terms in the equation of motion are the Lorentz force terms due to the dominant confining magnetic field $\vec{B}_\mathrm{o} = B_\mathrm{o}\vec{e}_\parallel$, and the electric field set by the charge separation, respectively. Both fields are static, the former is externally imposed and known (giving rise to fast cyclotron oscillation) while the latter needs to be evaluated.

The equation of motion and the continuity equation contain products of unknown functions. Hence usual linear equation solvers cannot be adopted to solve this set of equations. But an iterative scheme to solve them can be set up by gradually 'switching on' the nonlinearity. The reasoning is as follows:

(1) Solve the equation of motion analytically for a given set of forces in each iteration step.
(2) Average over the cyclotron period to remove the fast dynamics. This yields the drift velocity perpendicular to the static magnetic field.
(3) Find a suitable expression for the parallel velocity.
(4) Substitute the velocity information in the continuity equation to get an equation for the density.
(5) Introduce the obtained ion and electron densities in Poisson's equation.
(6) Solve the system of equations iteratively by updating the force terms involving the density and the potential in the equation of motion at each iteration step.

More explicitly: for a given static acceleration $\vec{a} = -v_\mathrm{t}^2[\nabla N]/N - q\nabla\Phi/m$ apart from the strong acceleration imposed by the confining magnetic field, the solution of the equation of motion is

$$v_+ = v_{+0}\exp[-\mathrm{i}\Omega t] + \frac{a_+}{-\mathrm{i}\Omega}$$
$$v_- = v_{-0}\exp[+\mathrm{i}\Omega t] + \frac{a_-}{+\mathrm{i}\Omega},$$

(where $v\pm = v_{\perp,1} \pm \mathrm{i}v_{\perp,2}$) which consists of a rapidly varying contribution oscillating at the cyclotron frequency, and a slow drift term across the magnetic field lines of the usual form $\vec{v}_{\mathrm{drift},\perp} = [\vec{a}\times\vec{e}_\parallel]/\Omega$.

The magnetic field does not influence the parallel dynamics and thus the $\vec{B}_\mathrm{o} = 0$ method can be applied to capture the parallel dynamics. Whereas the magnetic field causes a rapid cyclotron gyration that never loses its time dependence, the pressure and the electrostatic potential allow one to set up a stationary state flow. One obtains

$$v_\parallel\frac{\partial}{\partial x_\parallel}v_\parallel = -\frac{v_t^2}{N}\frac{\partial N}{\partial x_\parallel} - \frac{q}{m}\frac{\partial\Phi}{\partial x_\parallel} \tag{2}$$

which can easily be solved to yield

$$N(\vec{x}) = N(\vec{x}_\perp, x_{\parallel,0})\exp\left[-\frac{1}{v_t^2}\left[\frac{v_\parallel^2}{2} + \frac{q}{m}\Phi\right]\right]. \tag{3}$$

Seeking the static density setup close to the wall, the latter can be introduced in the steady-state continuity equation which yields an expression allowing one to evaluate the density of each of the species

$$N\nabla_\perp\cdot\vec{v}_{\mathrm{drift},\perp} + N\frac{\partial v_\parallel}{\partial x_\parallel} + \vec{v}_{\mathrm{drift},\perp}.\nabla_\perp N + v_\parallel\frac{\partial N}{\partial x_\parallel} = 0$$

in which the parallel velocity derivative is easily substituted for a density derivative using equation (2). Since $\nabla_\perp\cdot\vec{v}_{\mathrm{drift},\perp} = 0$, one finds

$$v_\parallel\vec{v}_{\mathrm{drift},\perp}\cdot\nabla_\perp N + [v_\parallel^2 - v_t^2]\frac{\partial N}{\partial x_\parallel} - \frac{Nq}{m}\frac{\partial\Phi}{\partial x_\parallel} = 0.$$

The above involves derivatives in various directions. Assuming that the dynamics in the direction perpendicular to the wall is dominant while the changes in the other two directions can be captured by simply taking $\partial/\partial y \approx \lambda_y$ and $\partial/\partial z \approx \lambda_z$ for the density, parallel velocity and potential, this equation can finally be cast in a form that makes the x-dependence explicit. The resulting equation is

$$\begin{aligned}&\left[v_\parallel[v_{\mathrm{drift},\perp 1}\mathcal{R}_{2,1} + v_{\mathrm{drift},\perp 2}\mathcal{R}_{3,1}] + [v_\parallel^2 - v_t^2]\mathcal{R}_{1,1}\right]\frac{\partial N}{\partial x}\\ &+\Big[v_\parallel[v_{\mathrm{drift},\perp 1}(\mathcal{R}_{2,2}\lambda_y + \mathcal{R}_{2,3}\lambda_z) + v_{\mathrm{drift},\perp 2}(\mathcal{R}_{3,2}\lambda_y\\ &+\mathcal{R}_{3,3}\lambda_z)] + [v_\parallel^2 - v_t^2](\mathcal{R}_{1,2}\lambda_y + \mathcal{R}_{1,3}\lambda_z)\Big]N\\ &-\frac{qN}{m}\left[\mathcal{R}_{1,1}\frac{\partial\Phi}{\partial x} + (\mathcal{R}_{1,2}\lambda_y + \mathcal{R}_{1,3}\lambda_z)\Phi\right] = 0.\end{aligned} \tag{4}$$

Rewriting equation (2) for the parallel dynamics in terms of x coordinate results in

$$\begin{aligned}&v_\parallel\left[\mathcal{R}_{1,1}\frac{\partial}{\partial x}v_\parallel + (\mathcal{R}_{1,2}\lambda_y + \mathcal{R}_{1,3}\lambda_z)v_\parallel\right]\\ &= -v_t^2\left[\frac{\mathcal{R}_{1,1}}{N}\frac{\partial N}{\partial x} + (\mathcal{R}_{1,2}\lambda_y + \mathcal{R}_{1,3}\lambda_z)\right] - \frac{q}{m}\left[\mathcal{R}_{1,1}\frac{\partial\Phi}{\partial x}\right.\\ &\left.+(\mathcal{R}_{1,2}\lambda_y + \mathcal{R}_{1,3}\lambda_z)\Phi\right].\end{aligned} \tag{5}$$

Finally, the relevant Poisson equation can be written as

$$\frac{\partial Y}{\partial x} = -(\lambda_y^2 + \lambda_z^2)\Phi + \frac{e}{\epsilon_o}\left[N_\mathrm{e} - \sum_i Z_\mathrm{i}N_\mathrm{i}\right], \tag{6}$$

$$\frac{\partial\Phi}{\partial x} = Y. \tag{7}$$

The obtained system of four first order equations can be solved iteratively, adopting the density, parallel velocity, potential and potential derivative of the previous iteration when computing a new estimate. When the various quantities do no longer vary from one iteration to the next, the solution of the nonlinear problem has been found. Note that the adopted procedure implicitly relies on the magnetic field being strong so that the cyclotron motion and the slow variation occur on two well

separated time scales. Also the convergence of the scheme relies on the iteration scheme chosen. In practice one can start the integration at $x_{\rm plasma}$ well away from the metallic wall imposing a given density $N_{\rm e} = \sum_i Z_{\rm i} N_{\rm i}$ while also taking $\Phi = 0$ there. Since only asymptotically far away from the wall charge neutrality is truly recaptured, it makes sense to also impose a small but finite value of $\partial\Phi/\partial x$ at $x_{\rm plasma}$; another option is to assume that the voltage applied to the wall is known and to impose that value at $x_{\rm wall}$. Lacking proper information on what the voltage at the wall is, it was preferred not to constrain it via the boundary conditions, i.e. to keep it floating. Finally, a velocity guess needs to be chosen at a reference point. In the sheath computation example in this paper, a single ion species is considered and $v_{\rm e} = Z_{\rm i} v_{\rm i}$ is chosen at $x_{\rm plasma}$ to ensure no net current flows in the plasma well away from the wall; $v_{\rm i}$ is taken to be of the order of the ion thermal velocity but slightly larger.

The model in this appendix is merely meant to reproduce the main features of the density variation in the sheath, the density being considered as an input to the fast time scale wave equations. Only qualitative reproduction of the proper density profile is sought, and clearly the adopted model should be refined. It was discussed in section 2 that the proper modeling of how the density profile in the presence of a strong magnetic field and close to metallic objects is set up is a rather delicate subject. Here, the discussion of the best choice of boundary conditions is left aside based on the purely mathematical statement that the same solution of a differential equation can be obtained via various boundary conditions, as long as these sets of boundary conditions are consistent with one another. For Poisson's equation this can be carried out by imposing the value of the potential or of its derivative at two reference points, or by imposing the potential and the derivative at either the same or two different positions. It is useful to remind that the Poisson equation solved does in no way account for the impact the rapidly varying electric field has on the slow time scale, i.e. that the coupling of the two times scales is not yet addressed in this paper.

Note the present set of equations adds further dynamics to the electrons: whereas they are assumed to rigorously satisfy the Boltzmann relation in many papers on sheath dynamics, the velocity convection term $\vec{v}\cdot\nabla\vec{v}$ has now been kept since a stationary state solution requires $\partial/\partial t = 0$ but not $\mathrm{d}/\mathrm{d}t = 0$. In spite of the fact that the chosen finite electron velocity is small with respect to the electron thermal velocity it plays a non-negligible role in the sheath dynamics: the electron density is not a simple relation linking the temperature, the potential and the density arising from the balance of the pressure and the electric field term in the equation of motion but it also involves the velocity and cannot be solved by hand in general. Apart from the need to specify boundary conditions for the potential and density, a proper choice for the velocity at either the wall or the interface of the sheath with the plasma needs to be provided and will have its influence on the density profile that will be set up in the sheath. An *a priori* assumption on the magnitude of the velocity restricts the applicability of the equations describing the sheath, while keeping the term allows one to study when it can justifiably be neglected and constitutes a firmer approach. Being a minor correction to the potential appearing in equation (3) for the electrons as the flow velocity is small compared with the thermal velocity for the electrons, the electron flow velocity term is non-negligible compared with the ion speed and this is crucial in the expression of the current density $\vec{J} = \sum_{\alpha={\rm e,i}} q_\alpha N_\alpha \vec{v}_\alpha$.

It is clear from the discussion in section 2 of the main text that the dynamics of the sheath should be described much more accurately than is done via the here proposed method: effects such as recycling and sputtering from the wall, and secondary emission will determine the exact interaction between the electrostatic potential, the plasma species and the metallic wall. Such a study is not included in this paper which only addresses the cross-talk of wave solutions when charge neutrality is violated and when sheaths are formed on a length scale of the order of the Debye length. For example Kohno *et al* [20] demonstrated that the wave dynamics on the fast time scale critically depend on the input of the slow time scale. For what concerns the slow time dynamics, this paper limits itself to listing a number of aspects that certainly need to be accounted for when aiming at a more realistic model of the wave–plasma interaction in the sheath.

Figure 10 shows the formation of a sheath in a D plasma with a density of $10^{16}\,\mathrm{m}^{-3}$ and $T_{\rm D} = T_{\rm e} = 15\,\mathrm{eV}$; the magnetic field strength is 3.45 T while $\alpha = \beta = 0.5\,\mathrm{rad}$. For these parameters the Debye length is $2.88\times10^{-4}\,\mathrm{m}$. The top figure shows the ion and electron densities, the middle figure the parallel velocity, and the bottom figures the potential and its derivative. Consistent with sheath theory, the sheath occurs in a narrow layer of a few Debye lengths; the integration interval taken is 6 Debye lengths wide. Although the voltage change is modest, the corresponding electric field strength close to the wall is significant. This results in an acceleration of the ions and a depopulation of the wall region. Although very localized, the decrease is gradual and is not well represented by a 'depopulated gap' for the electrons, nor by a constant density for the ions.

In figure 11 the density profiles are shown for various densities at $x_{\rm plasma}$ ranging from 10^{15} to $10^{18}\,\mathrm{m}^{-3}$. At higher densities, the relative decrease in the density compared with its value well away from the metallic wall is more localized to the edge (a direct consequence of the shrinking Debye length) while the density depletion is more modest. For otherwise identical parameters the density depletion is a rather sensitive function of the edge temperature.

The static magnetic field in tokamaks is so large that the perpendicular drift velocity hardly plays a role in the sheath dynamics, to the exception of the case where $\mathcal{R}_{11}$ is so small ($B_{\rm o}$ almost perpendicular to $\vec{e}_x$) that the sheath dynamics is no longer dominated by the parallel dynamics; already in their early work [5, 6], Myra and D'Ippolito mentioned the importance of this limit where the electrons no longer have a sufficient movement normal to the wall to be able to create a sheath. Also the dynamics along the metallic wall is commonly not crucial in the equations unless there is reason to believe that λ_y or λ_z is locally large, which makes the adopted approximate approach to account for the tangential derivatives inappropriate whatsoever. Hence, when adopting

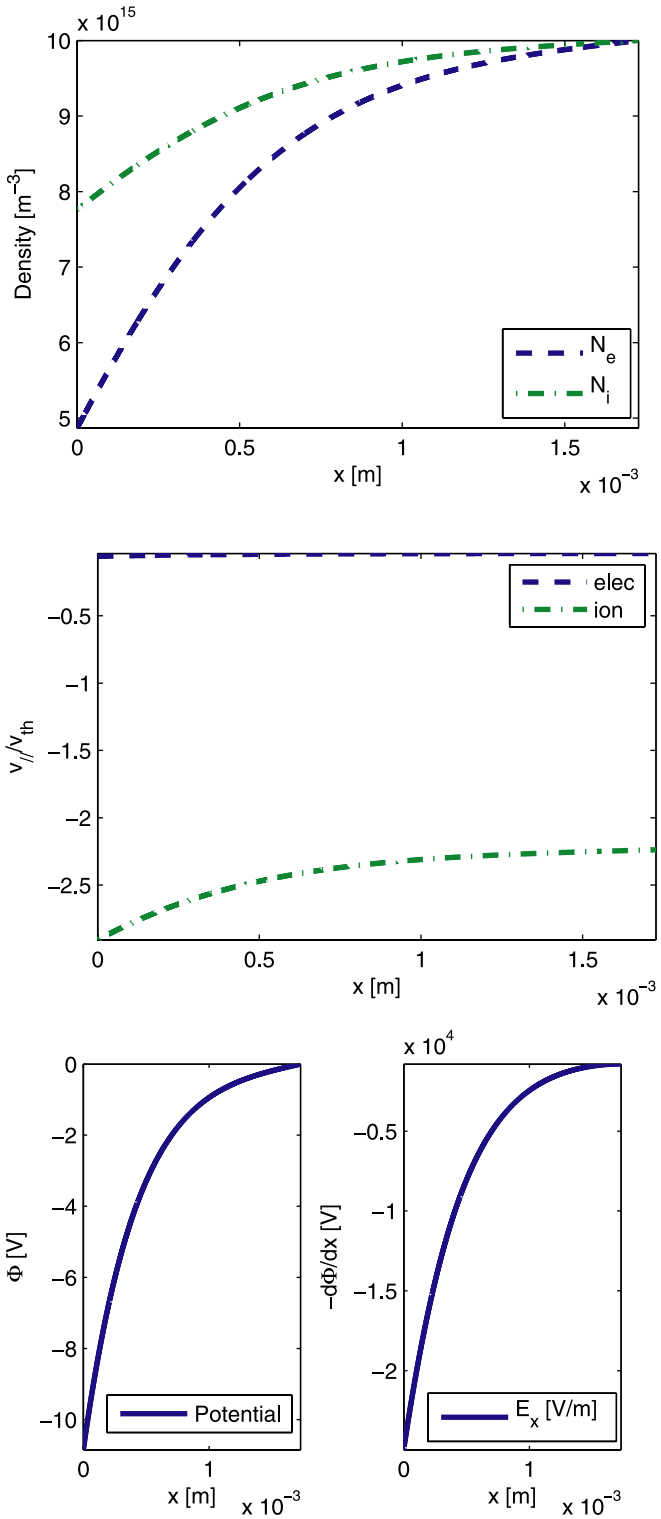

Figure 10. Sheath formation at a metallic wall as resulting from the approximate model discussed in the appendix; $N_e(x_{ref}) = 10^{16}\,m^{-3}$, $T_D(x_{ref}) = T_e(x_{ref}) = 15\,eV$, $B_o = 3.45\,T$, $\alpha = \beta = 0.5\,rad$. The wall is at $x = 0$ and the plasma edge of the integration interval x_{plasma} is 6 Debye lengths to the right. Here $\Phi = 0$, $Y = 800\,V\,m^{-1}$ and $v_{\|,i} = -6 \times 10^4\,m\,s^{-1}$ ($|v_{\|,i}| > v_{Bohm}$).

a local slab strategy the density consistent with the charge separation due to the presence of the metallic wall can in most cases qualitatively be captured by solving the simpler $\vec{B}_o = 0$ equation.

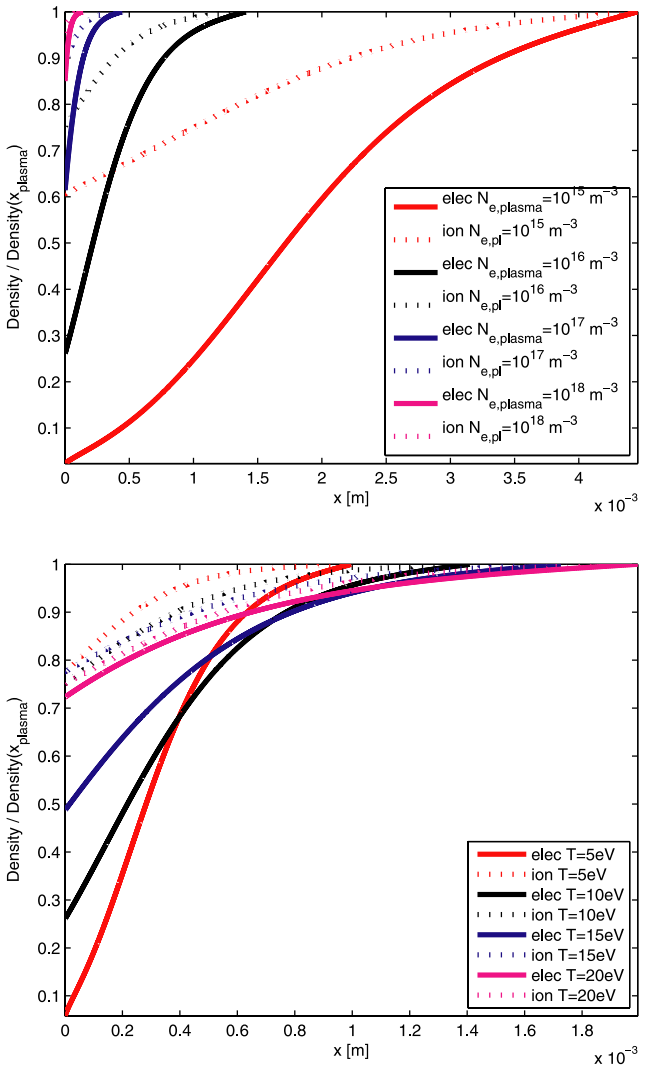

Figure 11. Sheath formation at a metallic wall; parameters as in the previous figure but for various densities (top) and temperatures (bottom) at the plasma side edge of the integration layer. Although plotted on a common x-axis, the integration interval width is fixed at 6 Debye lengths for each case.

The equations treated in this appendix are just the standard fluid equation, be it rewritten to set apart the effect of the magnetic field. The work is similar to the fluid expressions provided by Chodura [30] but the full equation of motion for the electrons is kept while Chodura considers the small velocity limit. The advantage of Chodura's procedure is that it allows one to write down a wave dispersion equation and identify the various possible modes for the slow time scale problem. The disadvantage is that it omits the convection term that is essential to grasp the role played by momentum in the sheath. As discussed in sections 2 and 5, the work of rigorously modeling RF sheaths in the presence of strong magnetic field is far from finished.

References

[1] Callen J D 2003 *Fundamentals of Plasma Physics* (Madison, WI: University of Wisconsin) http://homepages.cae.wisc.edu/~callen/book.html

[2] Jacquet Ph *et al* 2012 *20th Int. Conf. on Plasma Surface Interactions (Aachen, 21–25 May)* EFDA-JET-CP(12)02/01 P1-020
[3] Bobkov V *et al* 2012 *20th Int. Conf. on Plasma Surface Interactions (Aachen, 21–25 May)* EFDA-JET-CP(12)02/22 O3
[4] Perkins F W 1989 *Nucl. Fusion* **29** 583
[5] Myra J *et al* 1990 *Nucl. Fusion* **30** 845
[6] Myra J R *et al* 1994 *Phys. Plasmas* **1** 2891
[7] D'Ippolito D A *et al* 1998 *Nucl. Fusion* **38** 1543
[8] D'Ippolito D A *et al* 2006 *Phys. Plasmas* **13** 102508
[9] D'Ippolito D A 2008 *Phys. Plasmas* **15** 102501
[10] D'Ippolito D A *et al* 2009 *Phys. Plasmas* **16** 022506
[11] D'Ippolito D A *et al* 2010 *Phys. Plasmas* **17** 072508
[12] D'Ippolito D A *et al* 2011 *J. Nucl. Mater.* **415** S1001
[13] D'Ippolito D A 2012 *Phys. Plasmas* **19** 034504
[14] Jacquot J *et al* 2012 *39th EPS Conf. and 16th Int. Congress on Plasma Physics (Stockholm, 2–6 July), Europhysics Conf. Abstracts* vol 36F paper P2.038
[15] Colas L *et al* 2007 *Plasma Phys. Control. Fusion* **49** B35
[16] Louche F *et al* 2011 *Nucl. Fusion* **51** 103002
[17] Lamalle P U *et al* 2003 *30th EPS Conf. on Controlled Fusion and Plasma Physics (St. Petersburg, 7–11July)* vol 27A (ECA) P-1.193
[18] Van Eester D *et al* 2013 *Plasma Phys. Control. Fusion* **55** 025002
[19] Riyopoulos S 1999 *Phys. Rev.* E **59** 1111
[20] Kohno H, Myra J R and D'Ippolito D A 2012 *Comput. Phys. Commun.* **183** 2116
[21] Kohno H, Myra J and D'Ippolito D A 2012 *Phys. Plasmas* **19** 012508
[22] Colas L *et al* 2012 *Phys. Plasmas* **19** 092505
[23] Godyak V A *et al* 1990 *Phys. Rev.* A **42** 2299–2312
[24] Kim H C *et al* 2005 *Japan. J. Appl. Phys.* **44** 1957–1958
[25] Vahedi V *et al* 1993 *Plasma Sources Sci. Technol.* **2** 273
[26] Godyak V A *et al* 1990 *Phys. Rev. Lett.* **65** 996
[27] Stangeby P C 2012 *Nucl. Fusion* **52** 083012
[28] Zhang Z *et al* 2012 *Plasma Phys. Control. Fusion* **54** 082001
[29] Valsaque F *et al* 2001 *J. Nucl. Mater.* **290–293** 763–7
[30] Chodura R 1982 *Phys. Fluids* **25** 1628
[31] Manfredi G *et al* 2011 *Plasma Phys. Control. Fusion* **53** 015012
[32] Devaux S *et al* 2006 *Phys. Plasmas* **13** 083504
[33] Yankun J 2011 *Plasma Sci. Technol.* **13** 519
[34] Devaux S *et al* 2008 *Plasma Phys. Control. Fusion* **50** 025009
[35] Liu J-Y *et al* 2006 *Vacuum* **80** 1206
[36] Stix T H 1992 *Waves Plasmas* (New York: Springer)
[37] Swanson D G 1989 *Plasma Waves* (New York: Academic)
[38] Lancellotti V *et al* 2006 *Nucl. Fusion* **46** S476
[39] Kyrytsya V *et al* 2012 *Europhysics Conf. Abstracts* vol 36F paper P2.041
[40] Crombé K *39th EPS Conf. and 16th Int. Congress on Plasma Physics (Stockholm, 2–6 July), Europhysics Conf. Abstracts* vol 36F paper P-4.045